Sample pretreatment. An aliquot of 400 μL plasma was transferred to a 5 mL glass tube and alkalinized with 400 μL of 0.1 M ammonium hydroxide adjusted to pH 10.5 with phosphoric acid. After vortexing briefly, 1.8 mL of an ethyl acetate–acetonitrile mixture (9:1, v/v), freshly prepared, was added to each tube. The tubes were vortexed vigorously at room temperature for 5 min and centrifuged at 2000 *g* at 4°C for 10 min. Then, 1.5 mL of the organic phase was transferred to a 2 mL tube and evaporated to dryness under a gentle stream of nitrogen at 40°C. Subsequently, the residue was reconstituted in 150 μL of solvent A (see 'Chromatography'). The resulting solution was washed with 1 mL *n*-hexane by vortexing for 10 s and centrifuging at 2000 *g* for 2 min. After eliminating the upper hexane layer, the non-hexane solution was filtrated through a 0.45 μm filter and transferred to an auto-sampler vial. Aliquots of 50 μL were injected into the HPLC unit.

Chromatography. Chromatography was performed using an integrated high-performance liquid chromatography (HPLC) unit, Integral 100Q (Applied Biosystems, Foster City, CA, USA), which consists of an automatic sample injector, a binary solvent delivery pump and a dual-wavelength ultraviolet detector. The analytical column was a Develosil Ph-UG-3 column (150 × 2.0 mm, 3 μm particle size; Nomura Chemical Co., Seto City, Japan) protected by a Develosil Ph-UG-S precolumn (10 × 1.5 mm; Nomura Chemical Co.). The temperature was maintained at 40°C using a Shodex column heater (Showa Denko Co., Tokyo, Japan). Analytical runs were processed by the Turbochrom software (version 3.01; Applied Biosystems).

The mobile phase consisted of a gradient of solvents A and B. Solvent A was a mixture of 34% (v/v) acetonitrile and 66% (v/v) 25 mM NaH_2PO_4 containing 6 mM sodium 1-hexanesulfonate and exactly adjusted to pH 5.1 with 25 mM Na_2HPO_4. Solvent B was composed of 64% (v/v) acetonitrile and 36% (v/v) 25 mM NaH_2PO_4 containing 6 mM sodium hexanesulfonate and adjusted to pH 5.3. Over the first 14.6 min of the run, 100% solvent A was delivered constantly, and then the proportion of solvent B was increased linearly from 0% to 30% over 2.0 min. From time 16.6 to 35.5 min, a mixture of 70% solvent A and 30% solvent B was used in an isocratic mode. The column was then rinsed with 100% solvent B for 4.5 min and semi-equilibrated with 100% solvent A for 6.8 min. The flow rate was maintained at 200 μL/min. Prior to use, solvents were passed through a 0.45 μm filter and degassed by helium sparging.

Absorbance was monitored at a dual wavelength: channel 1 was set at a wavelength of 212 nm through the run. For channel 2, the wavelength was set at 266 nm for the first 18.3 min, then switched to 239 nm automatically and switched back to 266 nm at the end of the run. APV, SQV and the other six analytes were detected at 266, 239 and 212 nm, respectively.

Method validation. The calibration was established over the range of 0.025–15 μg/mL for SQV and 0.05–15 μg/mL for the other analytes using seven spiked plasma samples. The calibration curve for each analyte was constructed by least-squares linear regression of the observed peak area vs the spiked concentration. Unknown concentrations of quality controls and patient samples were calculated from the linear regression equation of daily calibration curve for each analyte. The data analyses were performed using Turbochrom software (version 3.01; Applied Biosystems) on a Windows personal computer.

The accuracy and precision of the method were determined by assaying plasma samples spiked with the analytes at three different concentrations of 0.3, 2.1 and 12 μg/mL. Accuracy was defined as the percentage of deviation from the nominal concentration. Intra-assay precision was calculated as the relative standard deviation from six replicate quality controls within a single assay. Inter-assay precision was estimated from the analyses of quality controls on five separate days. The lower limits of quantitation (LLQs) were determined with plasma samples spiked with decreasing concentrations of the analytes (0.0125, 0.025, 0.05 and 0.1 μg/mL). The LLQ was defined as the lowest concentration for which the percentage deviation from the nominal concentration and the relative standard deviation were both less than 20%. The LLQ values were used for the lowest concentration of daily calibration curves. The upper limit of quantitation (ULQ) was arbitrarily determined as 15 μg/mL for each analyte.

The efficiency of the extraction procedure was determined with plasma samples spiked at three different concentrations of 0.3, 2.1 and 12 μg/mL in triplicate. The average recovery of each analyte was calculated by comparing the observed peak areas of the processed samples with those of non-processed standard solutions in mobile phase (solvent A). The stability of the analytes in plasma samples was investigated for three different conditions. Plasma was spiked with two concentrations of the analytes (0.3 and 12 μg/mL) and subsequently kept at 60°C for 60 min, 4°C for 7 days and −30°C for 60 days including three freeze–thaw cycles. These samples were analyzed together with freshly prepared samples and the ratios of the observed concentrations were calculated.

RESULTS

Representative chromatograms of plasma spiked with 1.8 μg/mL of each of the six PIs, NFV M8 and EFV are shown in Fig. 2. IDV, NFV M8, EFV, RTV, LPV and NFV were detected at a wavelength of 212 nm [Fig. 2(A)], based on their ultraviolet absorption spectra (data not shown). APV and SQV were monitored at 266 and 239 nm, respectively [Fig. 2(B)], because interfering endogenous peaks were observed near the peaks of these analytes at 212 nm. The retention times were 14.4, 16.2, 21.8, 23.7, 25.8, 30.0, 31.4 and 33.0 min for IDV, APV, NFV M8, EFV, SQV, RTV, LPV and NFV, respectively.

Blank plasma samples from eight healthy individuals showed no endogenous peaks interfering with any analyte. The typical chromatograms are presented in Fig. 3. A total of 35 drugs, which are frequently co-administered to HIV-infected patients, were also examined for possible analytical interference (Table 1). All the drugs but ketoconazole were eluted at retention times of <10 min or were not detected with the method. Ketoconazole had a retention time of 20.2 min,

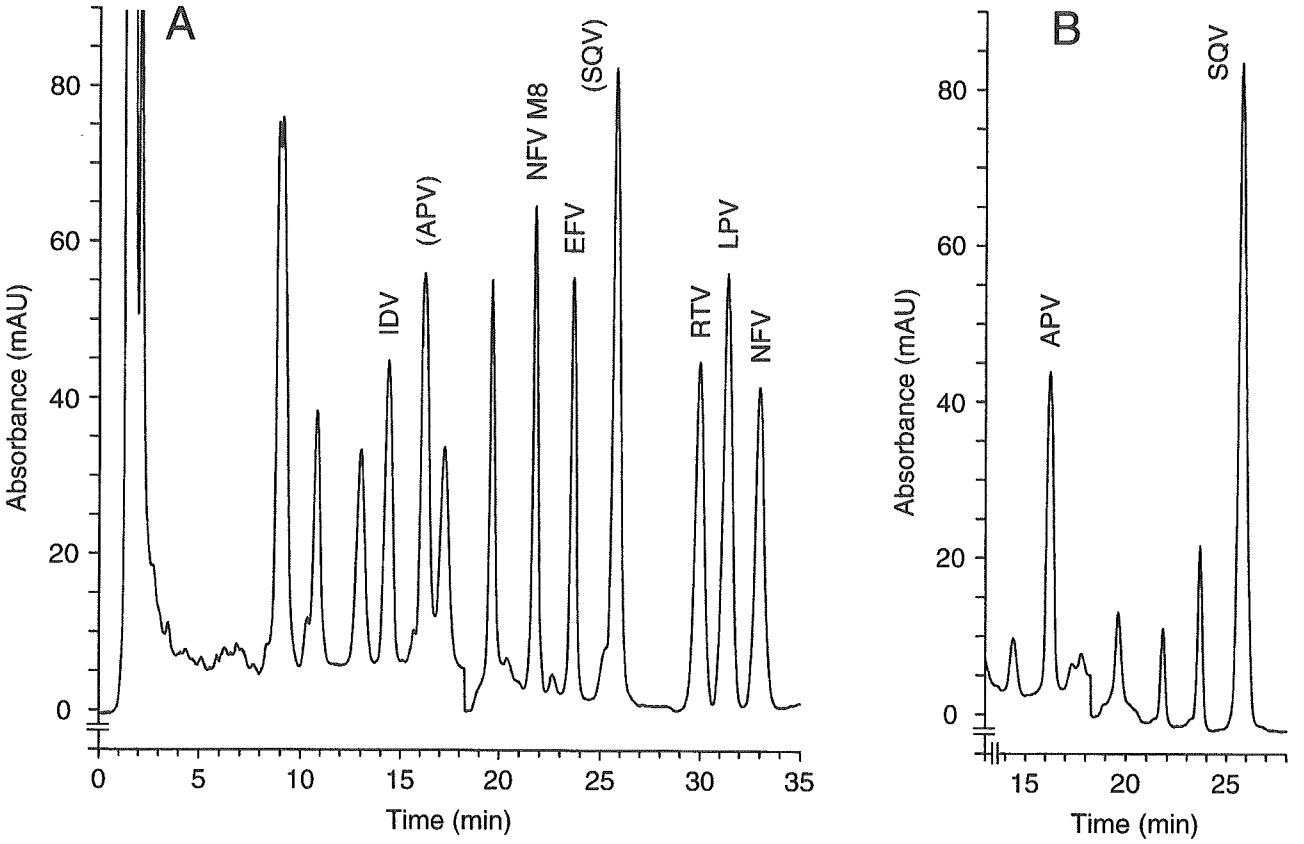

Figure 2. Chromatograms of a plasma sample spiked with 1.8 μg/mL of APV, EFV, IDV, LPV, NFV, NFV M8, RTV and SQV. Absorbance was monitored at 212 nm (A) and 266/239 nm (switched from 266 to 239 nm at 18.3 min) (B).

Table 1. Drugs tested for possible analytical interference

Abacavir	Erythromycin	Pentamidine
Acetaminophen	Ethambutol	Prednisolone
Aciclovir	Fluconazole	Pyrazinamide
Amikacin	Foscarnet	Rifampicin
Amoxicillin	Ganciclovir	Stavudine
Amphotericin B	Hydroxyurea	Sulfamethoxazole
Ampicillin	Isoniazid	Trimethoprim
Azithromycin	Kanamycin	Vancomycin
Cefaclor	Ketoconazole	Zalcitabine
Clarithromycin	Lamivudine	Zidovudine
Clindamycin	Metronidazole	Zidovudine glucuronide
Didanosine	Nevirapine	

which was obviously different from that of NFV M8 (21.8 min). Interference with metabolites of PIs and EFV was investigated with clinical samples, because these metabolites except NFV M8 are not available in pure form. No peaks interfering with any analyte were observed in plasma samples from patients receiving PIs and EFV (data not shown).

Over the concentration range 0.025–15 μg/mL for SQV and 0.05–15 μg/mL for the other seven analytes, the calibration curves were constructed by least-squares analysis. The correlation coefficients (r^2) of the curves were 0.995, 0.992, 0.998, 0.998, 0.997, 0.999, 0.998 and 0.999 for APV, EFV, IDV, LPV, NFV, NFV M8, RTV and SQV, respectively. The results of the accuracy and precision of the method are summarized in Table 2. The accuracies for the analytes at three concentration levels ranged from −6.9 to +7.6%. The intra-assay and inter-assay precisions were <9.2 and <11.8%, respectively. The LLQs were 0.025 μg/mL for SQV and 0.05 μg/mL for the other analytes, as determined with the plasma samples spiked with decreasing concentrations of the analytes. The ULQ was arbitrarily defined as 15 μg/mL for each analyte. The accuracies and precisions at the ULQ were also <20%.

The average extraction recoveries were 84.8, 70.9, 90.6, 88.3, 73.7, 80.0, 93.1 and 95.4% for APV, EFV, IDV, LPV, NFV, NFV M8, RTV and SQV, respectively. Although the reasons for the relatively lower recoveries of EFV and NFV are unclear, these had no negative effects on the assay performance as described above. The stability of the analytes in plasma samples is shown in Table 3. Under all conditions tested, the analytes proved to be stable with a recovery of >90.6% of the initial concentration.

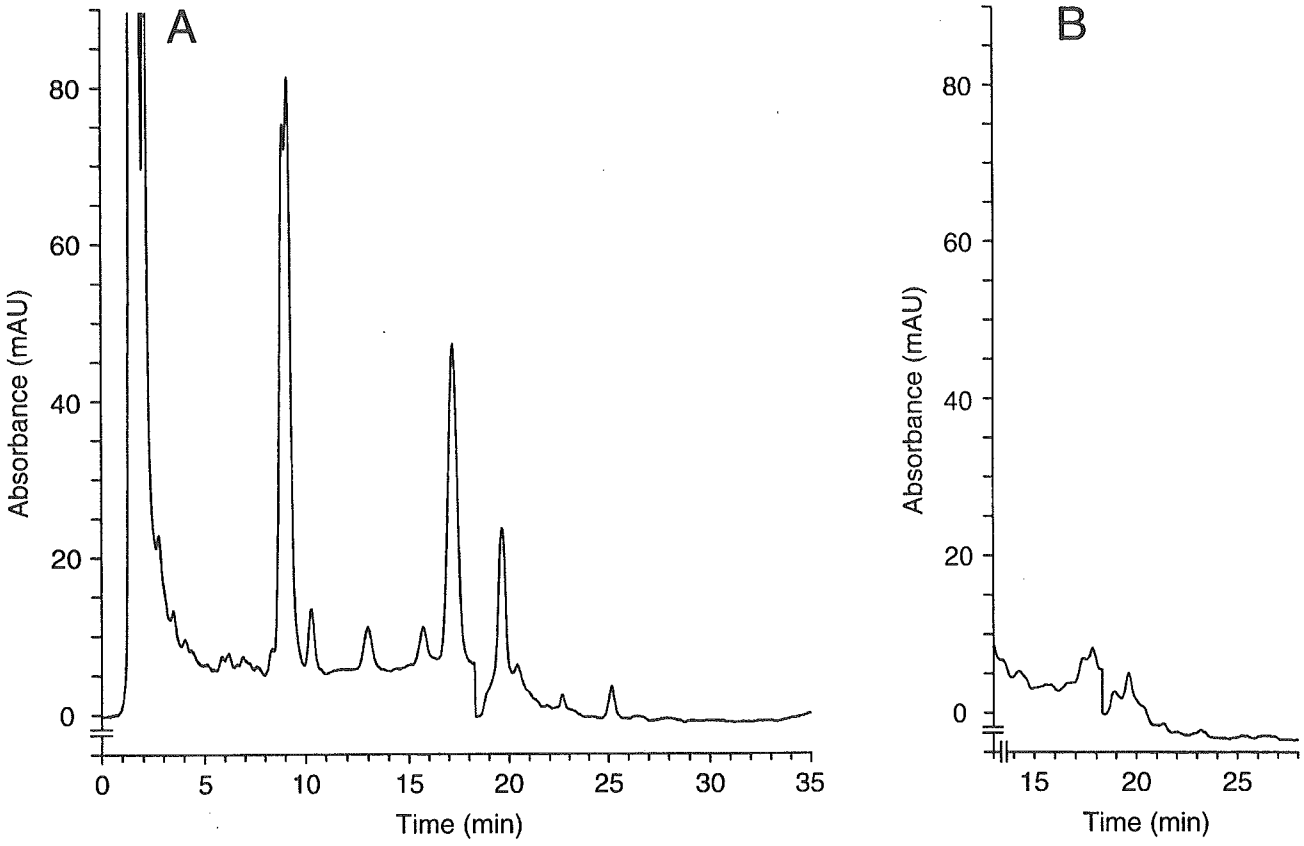

Figure 3. Chromatograms of a blank plasma sample. Absorbance was monitored at 212 nm (A) and 266/239 nm (switched from 266 to 239 nm at 18.3 min) (B).

Table 2. Accuracy and precision of the analytical method

Analyte	Concentration (μg/mL)	Accuracy (%)[a] (n = 6)	Precision (%)[b] Intra-assay (n = 6)	Precision (%)[b] Inter-assay (n = 5)
Amprenavir	0.3	+1.3	8.9	7.8
	2.1	−6.9	4.0	5.1
	12.0	+2.0	3.9	6.7
Efavirenz	0.3	+7.6	7.5	11.8
	2.1	−0.3	4.1	8.4
	12.0	+3.5	2.2	5.3
Indinavir	0.3	−2.0	6.1	9.0
	2.1	+1.7	3.1	4.9
	12.0	+5.2	5.4	4.3
Lopinavir	0.3	+4.5	5.6	9.5
	2.1	+2.8	4.0	6.1
	12.0	−0.9	4.3	5.9
Nelfinavir	0.3	+3.1	5.0	5.3
	2.1	+1.9	5.4	4.7
	12.0	−1.6	2.1	3.2
Nelfinavir M8	0.3	+4.4	4.6	6.7
	2.1	−0.3	2.9	4.4
	12.0	−1.6	1.5	3.6
Ritonavir	0.3	−2.0	9.2	7.3
	2.1	+3.2	3.8	5.1
	12.0	−4.1	3.1	5.9
Saquinavir	0.3	+1.7	3.9	2.8
	2.1	−0.2	2.2	3.4
	12.0	+3.1	4.2	4.7

[a] Deviation from nominal concentration.
[b] Relative standard deviation within a single assay or between different assays.

Table 3. Stability of protease inhibitors and efavirenz in plasma samples

Analyte	Concentration (μg/mL)	Recovery (%)[a] 60 min at 60°C (n = 3)	7 days at 4°C (n = 3)	60 days at −30°C with three freeze–thaw cycles (n = 4)
Amprenavir	0.3	94.7	104.8	95.6
	12.0	91.4	103.0	101.7
Efavirenz	0.3	95.8	100.7	98.8
	12.0	90.6	99.1	95.9
Indinavir	0.3	91.5	105.2	94.8
	12.0	93.2	100.8	98.6
Lopinavir	0.3	94.0	104.1	98.0
	12.0	93.3	101.3	100.5
Nelfinavir	0.3	102.4	102.5	99.8
	12.0	96.2	101.8	99.2
Nelfinavir M8	0.3	95.6	98.6	93.3
	12.0	98.1	101.8	97.6
Ritonavir	0.3	96.7	107.3	96.9
	12.0	93.2	103.0	97.2
Saquinavir	0.3	97.3	102.9	97.8
	12.0	92.8	102.6	100.4

[a] Compared with freshly prepared samples.

Table 4. Plasma concentrations of protease inhibitors and efavirenz in 10 patients

Patient no.	Drug	Dose (mg)[a]	Time after dosing (h)	Concentration (μg/mL)
1	Amprenavir	1200, b.i.d.	10.0	0.22
	Efavirenz	600, q.d.	10.0	0.53
2	Amprenavir	1200, b.i.d.	2.0	6.47
	Ritonavir	200, b.i.d.	2.0	0.38
	Efavirenz	600, q.d.	12.0	1.47
3	Indinavir	800, t.i.d.	6.5	0.19
4	Indinavir	400, b.i.d.	2.0	3.53
	Ritonavir	400, b.i.d.	2.0	2.55
5	Lopinavir	400, b.i.d.	3.0	5.94
	Ritonavir	100, b.i.d.	3.0	0.42
6	Lopinavir	400, b.i.d.	12.0	3.06
	Ritonavir	100, b.i.d.	12.0	0.09
7	Nelfinavir	1250, b.i.d.	4.5	1.01 (nelfinavir M8 0.96)
8	Nelfinavir	1250, b.i.d.	11.0	0.78 (nelfinavir M8 0.23)
9	Saquinavir	400, b.i.d.	3.5	1.49
	Ritonavir	400, b.i.d.	3.5	6.03
10	Saquinavir	400, b.i.d.	11.5	0.56
	Ritonavir	400, b.i.d.	11.5	1.30

[a] b.i.d., twice a day; q.d., once a day; t.i.d., three times a day.

The present method was applied to the determination of drug concentrations in clinical samples (Table 4 and Fig. 4). Plasma samples were randomly collected from 10 patients receiving PIs and EFV. All the samples could be analyzed with no technical difficulties. The observed concentrations were within the concentration ranges reported in literature (Khoo *et al.*, 2001; Acosta *et al.*, 2002; Back *et al.*, 2002; Van Heeswijk, 2002).

DISCUSSION

In this report, we describe the development, validation and clinical application of a novel chromatographic method for the simultaneous determination of the six widely used PIs and the most frequently used NNRTI, EFV, in plasma. To date, several methods have been reported for the simultaneous determination of different PIs or PIs plus NNRTIs (Leibenguth *et al.*, 2001;

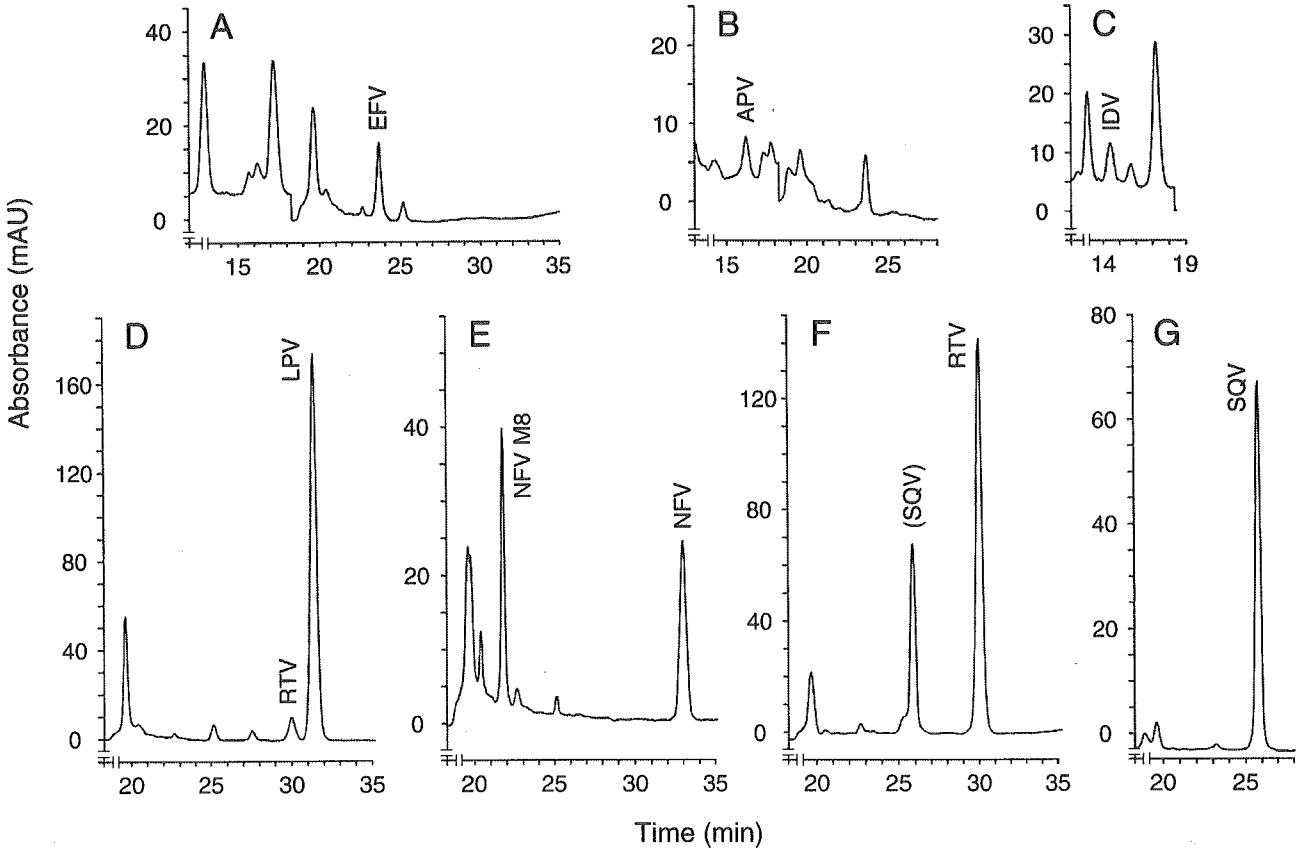

Figure 4. Chromatograms of plasma samples from patient 1 (A and B), patient 3 (C), patient 5 (D), patient 7 (E) and patient 9 (F and G). Absorbance was monitored at 212 nm (A, C, D, E and F) and 266/239 nm (switched from 266 to 239 nm at 18.3 min) (B and G). For details of the patients, see Table 4.

Poirier *et al.*, 2002; Titier *et al.*, 2002; Tribut *et al.*, 2002; Volosov *et al.*, 2002; Crommentuyn *et al.*, 2003; Frerichs *et al.*, 2003; Rentsch, 2003; Turner *et al.*, 2003; Rezk *et al.*, 2004). However, most of these methods have limitations in clinical application, including insufficient quantitation sensitivity, laborious sample pretreatment with solid-phase extraction, or use of expensive mass spectrometry. A simple, economical and reliable method that is performable with standard hospital laboratory equipment is desirable for routine TDM. The present method proved sufficiently sensitive to be used for TDM, because the LLQ values of the method for individual drugs were lower than the trough concentrations observed with treated patients and the target trough concentrations estimated from clinical and *in vitro* data (Khoo *et al.*, 2001; Acosta *et al.*, 2002; Back *et al.*, 2002; Van Heeswijk, 2002). The method was also accurate and precise over a wide range of drug concentrations as described. Chromatography, which was relatively time-consuming, could be fully automated with no need for technical supervision, since samples were stable for 24 h in the auto-sampler (data not shown). We utilized an ultraviolet detector, commonly used in hospital laboratories, but not expensive and sophisticated mass spectrometry. For the sample pretreatment, we chose liquid–liquid extraction, which is economical compared with solid-phase extraction. To simplify the experimental procedure, an internal standard was not used; nevertheless the method provided satisfactory validation results. Thus, this method would be suitable for routine TDM in conventional hospital laboratory settings.

Moreover, from a clinical point of view, this method is noteworthy for two reasons. First, this method covers most of key drugs currently used other than NRTIs. Since the standard treatment of HIV infection, HAART, consists of various combinations of anti-HIV drugs (Richman, 2001; British HIV Association Writing Committee, 2003; The Panel on Clinical Practices for Treatment of HIV Infection, 2004; Yeni *et al.*, 2004), it would be convenient to use TDM to measure plasma concentrations of several drugs simultaneously with a single method rather than to use each different method for each drug. Although NRTI concentrations cannot be determined with this method, NRTIs are pro-drugs that are converted to their active triphosphate forms within cells, and therefore TDM with plasma is considered less beneficial compared with PIs and NNRTIs,

which directly exert their antiviral effects (Back *et al.*, 2002). Secondly, this method allows the determination of the M8 metabolite of NFV as well as the parent NFV. NFV M8, which is produced by CYP 2C19 in the liver, is equipotent to the unchanged parent NFV against HIV *in vitro* (Zhang *et al.*, 2001), although almost all the metabolites of PIs and EFV have no obvious antiviral activity. The pharmacokinetics of NFV M8 would be also markedly affected by genetic background, drug interactions and hepatic dysfunction, leading to a wide inter-patient variability (Khaliq *et al.*, 2000). These findings suggest that measurement of the parent NFV plus its M8 metabolite in plasma would be preferable to that of the parent alone for TDM in NFV treatment.

TDM with this method is expected to contribute to the optimization of HIV treatment for individual patients through modification of dosage and assessment of adherence to treatment. This method would be also useful for studying the relationships between drug concentrations and efficacy or toxicity and for analyzing pharmacokinetics and drug interactions in heavily co-medicated patients. Such concentration-oriented approaches and studies are in progress in our hospital.

CONCLUSION

A simple, economical and reliable chromatographic method has been developed for the simultaneous determination of the six PIs, NFV M8 and EFV in plasma. This method would be useful for routine TDM and pharmacokinetic studies in patients receiving PIs and EFV.

Acknowledgments

The authors thank Hiroyuki Fukuda of Applied Biosystems Japan Ltd for helpful suggestions. The authors also thank Abbott Laboratories, Japan Tobacco Inc., Kissei Pharmaceutical Co., Merck & Co. and Roche Products for providing the reference compounds. This study was supported in part by Grants-in-Aid for AIDS research from the Ministry of Health, Labour and Welfare of Japan (H15-15100101), by the Japanese Foundation for AIDS Prevention, and by the Organization of Pharmaceutical Safety and Research (01-4).

REFERENCES

Acosta EP, Henry K, Baken L, Page LM and Fletcher CV. Indinavir concentrations and antiviral effect. *Pharmacotherapy* 1999; **19**: 708.

Acosta EP, Gerber JG and The adult pharmacology committee of the AIDS clinical trials group. Position paper on therapeutic drug monitoring of antiretroviral agents. *AIDS Research and Human Retroviruses* 2002; **18**: 825.

Back D, Gatti G, Fletcher C, Garaffo R, Haubrich R, Hoetelmans R, Kurowski M, Luber A, Merry C and Perno CF. Therapeutic drug monitoring in HIV infection: current status and future directions. *AIDS* 2002; **16**: S5.

Barry MG, Merry C, Lloyd J, Halifax K, Carey P, Mulcahy F and Back DJ. Variability in trough plasma saquinavir concentrations in HIV patients: a case for therapeutic drug monitoring. *British Journal of Clinical Pharmacology* 1998; **45**: 501.

British HIV Association Writing Committee. BHIVA guidelines for the treatment of HIV-infected adults with antiretroviral therapy: July 2003; www.bhiva.org (access date: 18 October 2004).

Crommentuyn KML, Rosing H, Nan-Offeringa LGAH, Hillebrand MJX, Huitema ADR and Beijnen JH. Rapid quantification of HIV protease inhibitors in human plasma by high-performance liquid chromatography coupled with electrospray ionization tandem mass spectrometry. *Journal of Mass Spectrometry* 2003; **38**: 157.

Dresser GK, Spence JD and Bailey DG. Pharmacokinetic–pharmacodynamic consequences and clinical relevance of cytochrome P450 3A4 inhibition. *Clinical Pharmacokinetics* 2000; **38**: 41.

Fellay J, Marzolini C, Meaden ER, Back DJ, Buclin T, Chave JP, Decosterd LA, Furrer H, Opravil M, Pantaleo G, Retelska D, Ruiz L, Schinkel AH, Vernazza P, Eap CB and Telenti A. Response to antiretroviral treatment in HIV-1-infected individuals with allelic variants of the multidrug resistance transporter 1: a pharmacogenetics study. *Lancet* 2002; **359**: 30.

Frerichs VA, DiFrancesco R and Morse GD. Determination of protease inhibitors using liquid chromatography-tandem mass spectrometry. *Journal of Chromatography B* 2003; **787**: 393.

Gerber JG. Using pharmacokinetics to optimize antiretroviral drug-drug interactions in the treatment of human immunodeficiency virus infection. *Clinical Infectious Diseases* 2000; **30**: S123.

Hugen PW, Langebeek N, Burger DM, Zomer B, van Leusen R, Schuurman R, Koopmans PP and Hekster YA. Assessment of adherence to HIV protease inhibitors: comparison and combination of various methods, including MEMS (electronic monitoring), patient and nurse report, and therapeutic drug monitoring. *Journal of AIDS* 2002; **30**: 324.

Khaliq Y, Gallicano K, Seguin I, Fyke K, Carignan G, Bulman D, Badley A and Cameron DW. Single and multiple dose pharmacokinetics of nelfinavir and CYP2C19 activity in human immunodeficiency virus-infected patients with chronic liver disease. *British Journal of Clinical Pharmacology* 2000; **50**: 108.

Khoo SH, Gibbons SE and Back DJ. Therapeutic drug monitoring as a tool in treating HIV infection. *AIDS* 2001; **15**: S171.

Leibenguth P, Le Guellec C, Besnier JM, Bastides F, Mace M, Gaudet ML, Autret-Leca E and Paintaud G. Therapeutic drug monitoring of HIV protease inhibitors using high-performance liquid chromatography with ultraviolet or photodiode array detection. *Therapeutic Drug Monitoring* 2001; **23**: 679.

Marzolini C, Telenti A, Decosterd LA, Greub G, Biollaz J and Buclin T. Efavirenz plasma levels can predict treatment failure and central nervous system side effects in HIV-1-infected patients. *AIDS* 2001; **15**: 71.

Palella FJ Jr, Delaney KM, Moorman AC, Loveless MO, Fuhrer J, Satten GA, Aschman DJ and Holmberg SD. Declining morbidity and mortality among patients with advanced human immunodeficiency virus infection. *New England Journal of Medicine* 1998; **338**: 853.

Poirier JM, Robidou P and Jaillon P. Simultaneous determination of the six HIV protease inhibitors (amprenavir, indinavir, lopinavir, nelfinavir, ritonavir, and saquinavir) plus M8 nelfinavir metabolite and the nonnucleoside reverse transcription inhibitor efavirenz in human plasma by solid-phase extraction and column liquid chromatography. *Therapeutic Drug Monitoring* 2002; **24**: 302.

Rentsch KM. Sensitive and specific determination of eight antiretroviral agents in plasma by high-performance liquid chromatography-mass spectrometry. *Journal of Chromatography B* 2003; **788**: 339.

Rezk NL, Tidwell RR and Kashuba AD. High-performance liquid chromatography assay for the quantification of HIV protease inhibitors and non-nucleoside reverse transcriptase inhibitors in human plasma. *Journal of Chromatography B* 2004; **805**: 241.

Richman DD. HIV chemotherapy. *Nature* 2001; **410**: 995.

The Panel on Clinical Practices for Treatment of HIV Infection. Guidelines for the use of antiretroviral agents in HIV-1-infected adults and adolescents: March 23, 2004. AIDSinfo.nih.gov (access date: 18 October 2004).

Titier K, Lagrange F, Pehourcq F, Edno-Mcheik L, Moore N and Molimard M. High-performance liquid chromatographic method for the simultaneous determination of the six HIV-protease inhibitors and two non-nucleoside reverse transcriptase inhibitors in human plasma. *Therapeutic Drug Monitoring* 2002; **24**: 417.

Tribut O, Arvieux C, Michelet C, Chapplain JM, Allain H and Bentue-Ferrer D. Simultaneous quantitative assay of six HIV protease inhibitors, one metabolite, and two non-nucleoside reverse transcriptase inhibitors in human plasma by isocratic reversed-phase liquid chromatography. *Therapeutic Drug Monitoring* 2002; **24**: 554.

Turner ML, Reed-Walker K, King JR and Acosta EP. Simultaneous determination of nine antiretroviral compounds in human plasma using liquid chromatography. *Journal of Chromatography B* 2003; **784**: 331.

Van Heeswijk RP. Critical issues in therapeutic drug monitoring of antiretroviral drugs. *Therapeutic Drug Monitoring* 2002; **24**: 323.

Volosov A, Alexander C, Ting L and Soldin SJ. Simple rapid method for quantification of antiretrovirals by liquid chromatography–tandem mass spectrometry. *Clin. Biochem.* 2002; **35**: 99.

Yeni PG, Hammer SM, Hirsch MS, Saag MS, Schechter M, Carpenter CC, Fischl MA, Gatell JM, Gazzard BG, Jacobsen DM, Katzenstein DA, Montaner JS, Richman DD, Schooley RT, Thompson MA, Vella S and Volberding PA. Treatment for adult HIV infection: 2004 recommendations of the International AIDS Society—USA panel. *Journal of the American Medical Association* 2004; **292**: 251.

Zhang KE, Wu E, Patick AK, Kerr B, Zorbas M, Lankford A, Kobayashi T, Maeda Y, Shetty B and Webber S. Circulating metabolites of the human immunodeficiency virus protease inhibitor nelfinavir in humans: structural identification, levels in plasma, and antiviral activities. *Antimicrobial Agents and Chemotherapy* 2001; **45**: 1086.

Antiviral Chemistry & Chemotherapy 16:363–373

A novel small molecular weight compound with a carbazole structure that demonstrates potent human immunodeficiency virus type-1 integrase inhibitory activity

Hua Yan[1], Tomoko Chiba Mizutani[1], Nobuhiko Nomura[2], Tadakazu Takakura[2], Yoshihiro Kitamura[3], Hideka Miura[1], Masako Nishizawa[1], Masashi Tatsumi[1], Naoki Yamamoto[1] and Wataru Sugiura[1*]

[1]AIDS Research Center, National Institute of Infectious Diseases, Tokyo, Japan
[2]Research and Discovery Laboratories, Toyama Chemical Co. Ltd., Toyama, Japan
[3]Division of Infectious Diseases, Advanced Clinical Research Center, Institute of Medical Science, University of Tokyo, Japan.

*Corresponding author: Tel: +81 42 561 0771; Fax: +81 42 561 7746; E-mail: wsugiura@nih.go.jp

The integration of reverse transcribed proviral DNA into a host genome is an essential event in the human immunodeficiency virus type 1 (HIV-1) replication life cycle. Therefore, the viral enzyme integrase (IN), which plays a crucial role in the integration event, has been an attractive target of anti-retroviral drugs. Several IN inhibitory compounds have been reported previously, yet none has been successful in clinical use. To find a new, more successful IN inhibitor, we screened a diverse library of 12 000 small molecular weight compounds randomly by *in vitro* strand-transfer assay. We identified a series of substituted carbazoles that exhibit strand-transfer inhibitory activity at low micromolar concentrations. Of these, the most potent compound exhibited an IC_{50} of 5.00 ±3.31 μM (CA-0). To analyse the structural determinants of strand-transfer inhibitory activity of the carbazole derivatives, we selected 23 such derivatives from our compound library and performed further analyses. Of these 23 compounds, six showed strong strand-transfer inhibition. The inhibition kinetics analyses and ethidium bromide displacement assays indicated that the carbazole derivatives are competitive inhibitors and not intercalators. An HeLa4.5/LTR-nEGFP cell line was employed to evaluate *in vitro* virus replication inhibition of the carbazole derivatives, and IC_{50} levels ranged from 0.48–1.52 μM. Thus, it is possible that carbazole derivatives, which possess structures different from previously-reported IN inhibitors, may become novel lead compounds in the development of IN inhibitors.

Keywords: integrase inhibitor, carbazole, HIV-1, antiretroviral drug

Introduction

Human immunodeficiency virus type 1 (HIV-1), causative agent of acquired immunodeficiency syndrome (AIDS), possesses three critical enzymes for replication. These are protease (PR), reverse transcriptase (RT), and integrase (IN) (Ruscetti, 1985; Kohl *et al.*, 1988; LaFemina *et al.*, 1992). As inactivating any of these enzymes may negate the infectivity of HIV-1, the enzymes have been targets of anti-retroviral drug development. Indeed, great progress in anti-retroviral drug discovery has been achieved in recent decades, and today 10 RT inhibitors and eight PR inhibitors (De Clercq, 1992; Tronchet & Seman, 2003; Balzarini, 2004; Imamichi, 2004) are available for anti-retroviral treatments. The third enzyme, IN, has also been a major target of inhibitor development. L-708,906 and L-731,988, which possess diketo acid moieties within their structures, were the first IN-specific inhibitors discovered (Pommier *et al.*, 2000; Dayam & Neamati, 2003; Pluymers *et al.*, 2002; Hazuda *et al.*, 2000). S-1360 and L-870,810, which also have diketo acid moieties, are IN inhibitors that have reached clinical Phase I/II trials for the first time (Johnson *et al.*, 2004; Hazuda *et al.*, 2004). However, although there have been large advances in the development of IN inhibitors, further research and analysis is required to develop clinically usable compounds.

Integrase (IN), the leading target of novel anti-retroviral inhibitor development, is the enzyme responsible for integration, wherein reverse transcribed HIV-DNA is inserted into a host genome, and is critical for viral replication, which in turn establishes latency and chronic infection (Chun *et al.*, 1995). IN is composed of three distinct

domains – the N-terminal domain (amino acids 1–50) with a zinc-binding motif (Schauer & Billich, 1992; Burke *et al.*, 1992), the catalytic core domain (amino acids 50–212) with polynucleotidyl transfer activity and sequence-specific endonuclease activity (Engelman & Craigie, 1992; Engelman *et al.*, 1994) and the C-terminal domain (amino acids 212–288), which has been thought to relate to nonspecific DNA binding (Khan *et al.*, 1991; Woerner & Marcus-Sekura, 1993).

At present, the function and structure of each domain has not been fully understood. The most well-analysed domain is the catalytic core domain, and its active site has highly conserved amino acidic residues Asp64, Asp116 and Glu152, which are critical for polynucleotidyl transfer activity (LaFemina *et al.*, 1992; Engelman *et al.*, 1995). Previously reported potent IN inhibitors L-708,906, L-731,988, L-801,810, S-1360 and 5-CITEP are all targeted to this domain. These inhibitors bind to the active site, displace divalent metal ion Mg^{2+} from the active site and inactivate the catalytic activity of IN (Grobler *et al.*, 2002; Dayam & Neamati, 2003; Goldgur *et al.*, 1999; Johnson *et al.*, 2004). No specific inhibitors have been reported for the N-terminal and C-terminal domains.

In the present study we attempted to identify novel IN inhibitory compounds, and therefore we conducted a random screening of a library of small molecular weight compounds. As a result, we discovered a series of novel IN inhibitory compounds with carbazole structures, that are quite different from previously reported inhibitory compounds.

Materials and methods

Preparation of integrase

The sequence coding the NL4-3 integrase (IN) was cloned into pET28b(+) (Novagen, Madison, WI, USA), generating pET-IN that codes NL4-3 IN with a hexa-histidine tag at the N-terminus. *Escherichia coli* strain Rosetta (DE3) (Novagen) transformed with pET-IN was grown in 1 l of Super Broth (Biofluids, Camarillo, CA, USA) containing 100 μg/ml kanamycin at 30°C until the optical density of the culture had reached between 0.5 and 0.7 at 600 nm. The recombinant protein expression was induced by isopropyl-1-thio-D-galactopyranoside. After incubation for 3 h, the cells were harvested and resuspended in 100 ml of preparation buffer (20 mM Tris-HCl, pH 8.0, 0.5 M NaCl) and disrupted by sonication. Following high-speed centrifugation at 40 000×g for 45 min at 4°C, the pellet was homogenized in GBB buffer (50 mM Tris-HCl, pH 8.0, 6 M Guanidine HCl and 2 mM 2-ME). The residual pellet was again sonicated and centrifuged at 40 000×g for 30 min at 4°C.

The supernatant was filtered through a 0.22 μm filter and mixed with 1 ml of nickel-affinity resin (Sigma, St. Louis, MO, USA), and incubated overnight at 4°C. The resin was washed twice by mixing with 20 ml of GBB containing 5 mM imidazole (Sigma). The protein was eluted with GBB containing 1 M imidazole. The fractions containing integrase were pooled and 0.5 M EDTA was added to a final concentration of 5 mM. This eluted protein was then sequentially dialysed against (i) 6 M guanidine HCl, 50 mM Tris-HCl (pH 8.0), 2 mM 2-ME, 1 mM EDTA for 2 h at room temperature, (ii) 6 M guanidine HCl, 50 mM Tris-HCl (pH 8.0), 10 mM DTT, 1 mM EDTA for 16 h at room temperature, (iii) 4 M urea, 50 mM Tris-HCl (pH 8.0), 0.5 M NaCl, 1 mM DTT, 0.1 mM EDTA for 16 h at 4°C, (iv) 2 M urea, 50 mM Tris-HCl (pH 8.0), 0.5 M NaCl, 1 mM DTT, 0.1 mM EDTA, 20% (w/v) glycerol for 16 h at 4°C, (v) 1 M urea, 50 mM Tris-HCl (pH 8.0), 1 M NaCl, 1 mM DTT, 0.1 mM EDTA, 15 mM 3-[(3-cholamidopropyl) dimethylammonio]-1-propanesulfonate (CHAPS), 20% (w/v) glycerol for 16 h at 4°C, and (vi) 50 mM Tris-HCl (pH 8.0), 1 M NaCl, 1 mM DTT, 0.1 mM EDTA, 15 mM CHAPS, 20% (w/v) glycerol for 16 h at 4°C. The final preparation was stored at −80°C.

The purified enzyme activity was confirmed and evaluated by strand-transfer assay using M8 apparatus (IGEN, Gaithersburg, MD, USA).

Preparation of test compounds

A diverse library of 12 000 small-molecule compounds was supplied by Toyama Chemicals Co. Ltd. (Toyama, Japan). All test compounds were dissolved in DMSO and adjusted to 2 mM concentration. S-1360 was synthesized as positive control for strand transfer assay.

Construction of strand-transfer assay

Two different strand-transfer assay systems were employed in the IN inhibitor screening trial. For the first screening step, an M8 apparatus and strand-transfer assay kit, ORIGEN HIV integrase assay (IGEN), was used. In brief, magnetic beads coated with 29 mer donor double-stranded DNA (dsDNA) were mixed with purified IN (15 pmol), followed by adding the test compound and 20 mer target dsDNA tagged with ruthenium, conducting electronically inducible fluorescence chemistry, and incubating for 1 h at 37°C. Subsequently, the entire reaction solution was applied to the M8 apparatus, and then strand-transfer products were captured by a magnet in the flow-circuit of the equipment. The amount of the strand-transfer product was measured by ruthenium fluorescence activity. For the second and later screening steps, in-house strand-transfer assay was employed. The in-house assay was designed in 96-well plate format to achieve high-throughput screening.

The following donor and target DNA oligonucleotides were designed and used:
Donor-1 (D1): 5′-ACTGCTAGAGATTTTCCA-CACTGACTAAAAG-3′
Donor-2 (D2): Biotin-5′-CTTTTAGTCAGTGTGGA-AAATCTCTAGCA-3′
Target-1 (T1): 5′-CTAGAGATTTTCCACACTGACT-AAAAG-3′-Digoxigenin (DIG),
Target-2 (T2): 5′-CTTTTAGTCAGTGTGGAAAA-TCTCTAG-3′-DIG

To form dsDNA, the D1–D2 pair and the T1–T2 pair were mixed in the presence of 0.1 M NaCl and denatured for 10 min at 95°C, followed by an annealing process, gradual cooling down to room temperature. One pmol biotinulated donor dsDNA (D1–D2), 15 pmol IN protein and 5 µl test compounds (100 µM in DMSO) were mixed together in assay buffer (25 mM 3-(N-morpholino)-propanesulfonic acid, pH 7.2, 25 mM NaCl, 10 mM $MgCl_2$, 10 mM DTT, 5% PEG, 10% DMSO), followed by the addition of 0.75 pmol target dsDNA (T1–T2), and adjusted to a final volume of 100 µl and incubated for 1 h at 37°C. After the incubation, the mixture was adjusted to a final volume of 200 µl with ELISA buffer (20 mM Tris [pH 8.0], 0.4 M NaCl, 10 mM EDTA, 0.1 mg/ml sonicated DNA). To harvest the strand-transfer product, the mixture was transferred into a 96-well micro titre plate coated with streptavidin (PIERCE, Rockford, IL, USA), followed by adding an alkaline phosphatase conjugated anti-DIG antibody (Roche Diagnostics, Mannheim, Germany) and a disodium 3-(4-methoxyspiro{1,2-dioxetane-3,2′-(5′-chloro)tricyclo[3.3.1.1^{3,7}]decan}-4-yl) phenyl phosphate (CSPD) substrate (Roche). The lumino-intensity was quantified with a Luminous CT-9000D luminometer (DIA-IATRON, Tokyo, Japan).

In addition to the above two different strand-transfer assays, a strand-transfer assay with radioisotope labelled target DNA and SDS-PAGE was employed in order to visually confirm the strand-transfer inhibition (Craigie *et al.*, 1995). By use of T4 polynucleotide kinase (TAKARA BIO, Osaka, Japan), the 5′ end of 20 mer target oligonucleotide-A (5′-TGTGGAAAATCTCTAGCAGT-3′) was labelled with [γ-^{32}P] ATP (370 MBq/µl, Amersham Bioscience, Tokyo, Japan). After the labelling reaction was terminated by adding EDTA, complementary oligonucleotide-B (5′-ACTGCTAGAGATTTTCCACA-3′) was added, and dsDNA was formed by heat denaturation and gradual cooling to room temperature. Unincorporated [γ-^{32}P]ATP was removed by G-25 Column (Amersham Bioscience, Piscataway, NJ). The reaction products were applied to 20% denatured polyacrylamide gel electrophoresis (300V/25A). The result of the electrophoresis was analysed by BAS-2500 (Fuji film, Tokyo, Japan).

Inhibition kinetics of IN

To analyse the strand-transfer inhibition mechanism of the test compounds, whether the action is competitive inhibition or non-competitive inhibition, Michaelis-Menten constant (K_m) and maximum velocity (V_{max}) were evaluated. Strand-transfer inhibition was evaluated on eight different time points (0, 1, 3, 5, 7.5, 10, 15, and 20 min) with four different compound concentrations (0, 1, 5, 10 µM) and target DNA concentrations (0.167, 0.25, 0.5, and 1 pmol). The initial reaction rate constants of IN were determined by linear regression using linear data points of product concentration–time plots. K_m and V_{max} were calculated from the Y-axis intercept in a plot of the slopes of Lineweaver-Burk analysis.

Intercalative activity evaluation

To clarify the possibility of intercalative activity of test compounds, ethidium bromide (EtBr) displacement assay was carried out following the protocol reported previously (Cain *et al.*, 1978). In brief, 1 µM calf thymus DNA (Invitrogen, Carlsbad, CA, USA) was mixed with EtBr (final concentration at 1.26 µM) and reaction buffer (2 mM HEPES, 10 µM EDTA, 9.4 mM NaCl, pH 7.0), and incubated for 10 min at room temperature. After the incubation, test compounds were added into the calf thymus DNA–EtBr mixture at different concentrations (final concentrations of 0.01–1000 µM). Fluorescence intensity of each mixture was determined by Fluoroskan Ascent FL (Helsinki, Finland. Excited at 544 nm, emitted at 590 nm). Actinomycin D (ICN Biomedical, Aurora, OH, USA), which is known as an intercalator, was employed as the positive control of the assay.

Molecular modelling studies

Molecular modelling studies were carried out using SYBYL software Version 6.9.1 (Tripos, St. Louis, MO, USA) running on an SGI Fuel workstation equipped with 600-MHz R14000 processor (SGI, Mountain View, CA, USA).

Evaluation of *in vitro* antiviral activity.

To evaluate HIV-1 replication inhibition by selected test compounds, *in vitro* antiviral assays were performed using a HeLa4.5/nEGFP reporter cell line. The HeLa4.5/nEGFP reporter cell line was established by transfection of CD4 and LTR driven EGFP reporter protein into the HeLa cell line. HeLa4.5/nEGFP reporter cells were maintained with D-MEM (Sigma) containing 5% FCS (Hyclone, Logan, UT, USA), 500 µg/ml G418, 1 µg/ml blasticidin and 2 µg/ml puromycin.

One day before conducting the assay, $1x10^4$ HeLa4.5/nEGFP cells were seeded into clear bottom black 96-well plates (NUNC, Rochester, NY, USA) with

200 μl/well medium and incubated at 37°C, 5% CO_2. The next day, 1250 $TCID_{50}$ HXB2 were added in each well, followed by addition of the test compounds in final concentrations of 5, 1, 0.2, 0.04, 0.008, 0.0016, 0.00032, and 0.000064 μM. Forty-eight hours after infection, the cells were fixed by 3.2% formaldehyde and the nuclei of cells were stained by 10 μg/ml Hoechst33342 (Molecular Probes, Engene, OR, USA). EGFP positive cell number ($EGFP^+$) and Hoechst33342 positive cell number ($hoechst33342^+$) were determined by Cellomics Array Scan, HSC Systems (Beckman Coulter, Tokyo, Japan).

Inhibitory activity of each compound was determined by the following formula:

% inhibition = 1 − {($EGFP^+$ cell number with drug/$hoechst33342^+$ cell number with drug) − ($EGFP^+$ cell number without infection/$hoechst33342^+$ cell number without infection)}/{($EGFP^+$ cell number without drug/$hoechst33342^+$ cell number without drug) − ($EGFP^+$ cell number without infection/$hoechst33342^+$ cell number without infection)}.

Results

A small molecule bearing a carbazole moiety demonstrated strand-transfer inhibitory activity

A diverse library of 12 000 small-molecule compounds was screened for strand-transfer inhibitory activity at 100 μM concentration by M8 apparatus. Seventy-two compounds that demonstrated more than 80% strand-transfer-inhibition were selected and applied to the second screening using in-house strand-transfer assay. In the second screening, to confirm dose-dependent inhibition of the test compounds, each compound was tested at four different concentrations. Of the 72 compounds, a compound bearing a carbazole moiety, 8-chloro-2-[2-(dimethylamino)ethyl]-9-hydroxy-5-methylpyrrolo[3,4-c]carbazole-1,3(2H,6H)-dione (coded as **CA-0**), was found to demonstrate potent strand-transfer inhibitory activity (Figure 1A). As shown in Figure 1B, **CA-0** demonstrated clear dose-dependent inhibition of the strand-transfer reaction with an IC_{50} of 5.00 ±3.31 μM. The dose-dependent inhibition was also confirmed by SDS-PAGE with [γ-^{32}P] labelled target DNA. As demonstrated in Figure 1C, strand-transferred product bands diminished along with increased concentration of the inhibitor. IC_{50} value determined from intensities of the bands was 1.24 ±0.09 μM, which was consistent with that evaluated via the plate assay.

Strand-transfer inhibition of 23 carbazole derivatives, and the relationship between their structures and inhibitory activity

To understand the relationship between structure and strand-transfer inhibition activity, we selected 23 carbazole

Figure 1. Structure and strand transfer inhibitory activity of 8-chloro-2-[2-(dimethylamino) ethyl]-9-hydroxy-5-methylpyrrolo[3,4-c]carbazole-1,3(2H,6H)-dione (**CA-0**)

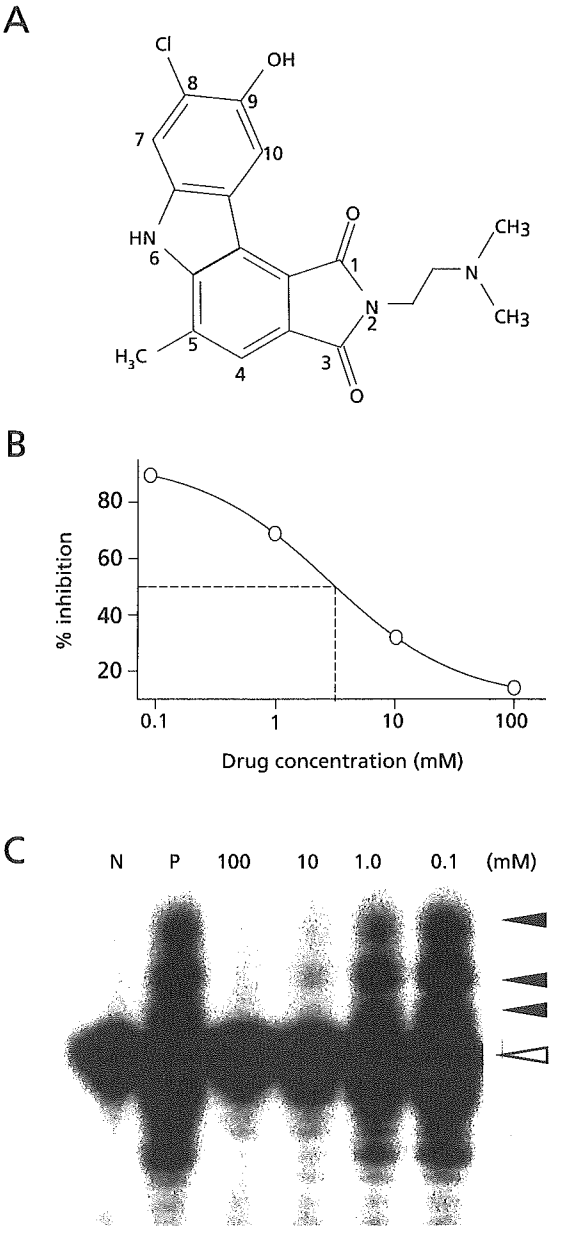

(A) The structure of **CA-0**, a strand transfer inhibitory compound identified from among a library of 12 000 small molecular weight compounds. It has a carbazole structure as a scaffold. The small numbers written beside the structure indicate the residue number of the compound. **(B)** A dose–response curve of **CA-0**. The dotted line indicates the IC_{50} point of the chemical, which was 5.00 ±3.31 μM. **(C)** A strand transfer assay by radioisotope-labelled oligonucleotide. Lane 1 "N" stands for the negative control, with only a radioisotope-labelled nucleotide. Lane 2 "P" stands for positive control, with radioisotope-labelled nucleotide and recombinant integrase. Lanes 3 to 6 were with inhibitor. The open triangle and solid triangle indicate labelled oligonucelotide and strand transfer products, respectively.

derivatives with different substituents. As demonstrated in Figure 2, all compounds had pyrrolo[3,4-c]carbazole structures as scaffolds, and all except **CA-5**, **CA-10** and **CA-19** had 2-dimethylaminoethyl group at position R2. Six of the 23 compounds demonstrated potent strand-transfer inhibition comparable to that of **CA-0**. These compounds were **CA-1**, **CA-4**, **CA-8**, **CA-9**, **CA-12** and **CA-13**. IC_{50} values of these test compounds were similar with positive control S-1360. Moderate inhibitory activities were observed in twelve compounds, **CA-2**, **CA-3**, **CA-7**, **CA-11**, **CA-14**, **CA-15**, **CA-16**, **CA-17**, **CA-18**, **CA-21**, **CA-22** and **CA-23**. Five compounds, **CA-5**, **CA-6**, **CA-10**, **CA-19** and **CA-20**, did not show significant inhibition, even at the highest concentration tested

Figure 2. Structures of **CA-0** and 23 carbazole derivatives evaluated for strand transfer inhibitory activity

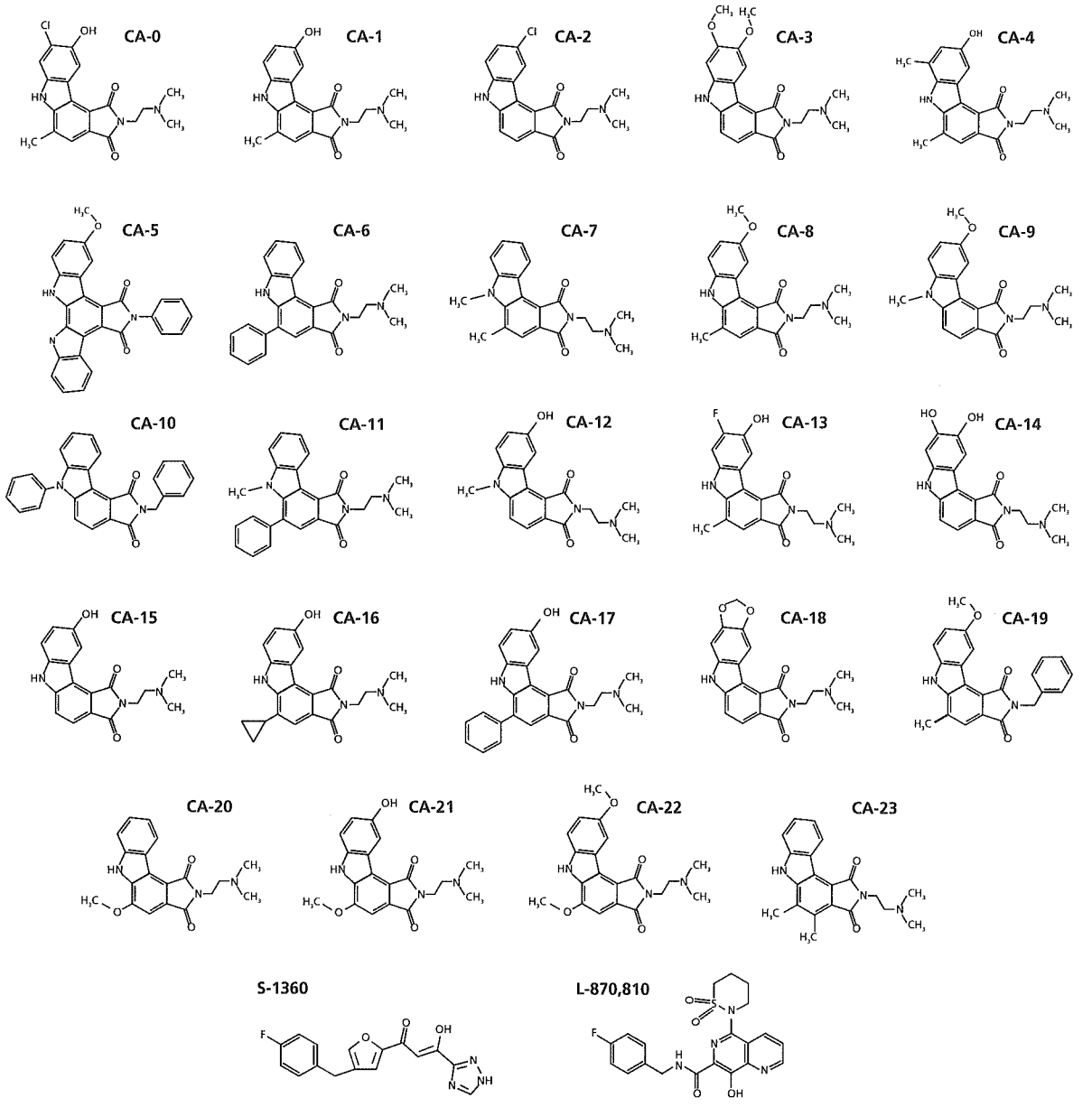

CA-0 and 23 related compounds with carbazole scaffold tested for strand-transfer inhibitory activities are depicted. S-1360 and L-870,810, which have previously been reported as potent IN inhibitors, are also shown.

(100 μM). The compounds that demonstrated potent strand-transfer inhibitory activity were also confirmed by gel-based assay, and IC_{50} values determined from the gel-based assay were consistent with the values determined via in-house plate assay (Table 1).

Carbazole derivatives are competitive inhibitors of integrase

To investigate the strand-transfer inhibitory mechanisms and kinetics of the compounds, we determined V_{max} and K_m of the inhibition by Lineweaver–Burke plot analyses. We selected two compounds, **CA-0** and **CA-13**, for the analyses. As summarized in Table 2, larger K_m values (nM) were observed with higher inhibitory concentration, whereas V_{max} values (RU/min) did not change and remained consistent at any inhibitory concentration (Figure 3). As shown in Figure 3A and 3B, data-fitted lines of different time points converged on the Y axis, indicating that **CA-0** and **CA-13** inhibited strand-transfer in a competitive manner.

Table 1. Strand transfer and *in vitro* viral replication inhibitory activities of carbazole derivatives

	IC_{50} in strand transfer assay		Anti-HIV activity
	Plate assay (μM)	Gel assay (μM)	IC_{50} (μM)
(A) High-inhibitory group			
CA-0	5.00 ±3.31	1.24 ±0.09	0.48 ±0.06
CA-13	4.38 ±2.78	1.13 ±0.21	0.51 ±0.12
CA-1	7.94 ±4.12	2.97 ±0.21	0.92 ±0.15
CA-4	8.99 ±3.39	6.34 ±0.89	1.52 ±0.46
CA-8	6.61 ±4.17	6.38 ±0.32	0.79 ±0.07
CA-9	4.42 ±1.87	4.10 ±0.46	0.80 ±0.11
CA-12	5.93 ±3.53	3.14 ±0.04	0.69 ±0.15
(B) Intermediate-inhibitory group			
CA-2	22.50 ±2.27	ND	ND
CA-3	72.69 ±5.44	ND	ND
CA-7	11.88 ±7.66	ND	ND
CA-11	57.00 ±3.13	ND	ND
CA-14	17.37 ±1.79	ND	ND
CA-15	27.28 ±9.10	ND	ND
CA-16	20.51 ±15.11	ND	ND
CA-17	50.64 ±19.02	ND	ND
CA-18	10.68 ±8.88	ND	ND
CA-21	25.01 ±10.60	ND	ND
CA-22	16.92 ±7.32	ND	ND
CA-23	16.94 ±7.82	ND	ND
(C) Intermediate-inhibitory group			
CA-5	>100	ND	ND
CA-6	>100	ND	ND
CA-10	>100	ND	ND
CA-19	>100	ND	ND
CA-20	>100	ND	ND
(D) Previously reported inhibitor			
S-1360	4.67 ±1.89	ND	ND

Underline, indicates original compound; IC_{50}, 50% inhibition concentration; ND, not done.

Carbazole derivates have not shown intercalative activity

Due to their planar structure and their manner of competitive inhibition, we were concerned that the compounds might have the intercalative activity to destroy substrate dsDNA, rather than binding to the IN to block its enzyme activity. To clear the possibility of the intercalation, EtBr displacement assay was carried out. Since EtBr intercalates into dsDNA and makes visualization possible by growing fluorescence under UV light, intercalative activity of the test compounds can be evaluated by whether the test compounds displace incorporated EtBr out from dsDNA. As shown in Figure 4, fluorescence intensity diminished in a dose-dependent manner by actinomycin D, a compound known as a potent intercalator. In contrast, our two test compounds **CA-0** and **CA-13** did not affect fluorescence intensity, even at the highest concentration of 1 mM, suggesting that **CA-0** and **CA-13** were not intercalators.

Antiviral activity

We employed a single replication infectivity assay using HeLa4.5/EGFP cells to investigate the potency of antiviral activity. IC_{50} values of **CA-0** and the six compounds were 0.48, 0.92, 1.52, 0.79, 0.8, 0.69, 0.51 μM, respectively. The IC_{50} values of all seven compounds were 5.5 to 10.4-fold lower than that of the strand transfer assay (Table 1A). The discrepancy in IC_{50} between the two assays can be explained by stoichiometry of the inhibitor and the target enzyme in the two assays, and the estimated amount of IN in-strand transfer assay was higher than in the

Table 2. Inhibition kinetics of representative carbazole compounds **CA-0** and **CA-13**

Chemical	Concentration	V_{max} (RU/min)	K_m (nM)
CA-0	10 μM	463.16 ±63.16	30.40 ±7.80
	5 μM	402.58 ±32.21	26.21 ±7.40
	1 μM	370.14 ±84.42	12.71 ±2.02
	0 μM	454.55 ±0.02	9.18 ±1.18
CA-13	10 μM	409.70 ±35.47	19.31 ±4.68
	5 μM	439.07 ±164.74	14.83 ±0.24
	1 μM	438.08 ±53.85	11.09 ±2.42
	0 μM	429.83 ±136.46	7.08 ±0.64

Figure 3. Inhibition kinetics assays of two representative carbazole derivatives, **CA-0** and **CA-13**

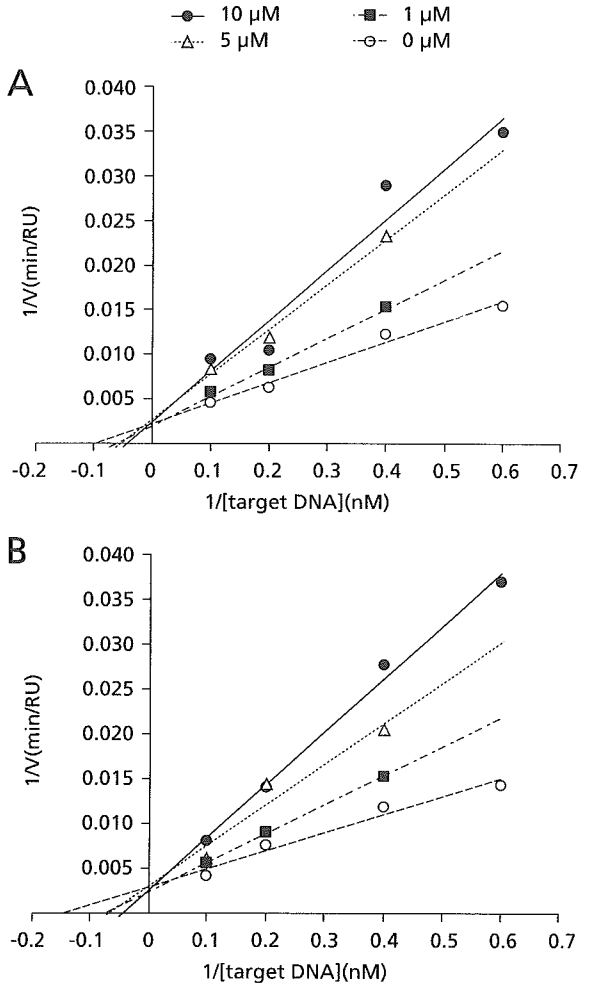

Lineweaver–Burke plot analyses of **(A) CA-0** and **(B) CA-13** are depicted.

Figure 4. Ethidium bromide displacement assays of two representative carbazole derivatives, **CA-0** and **CA-13**

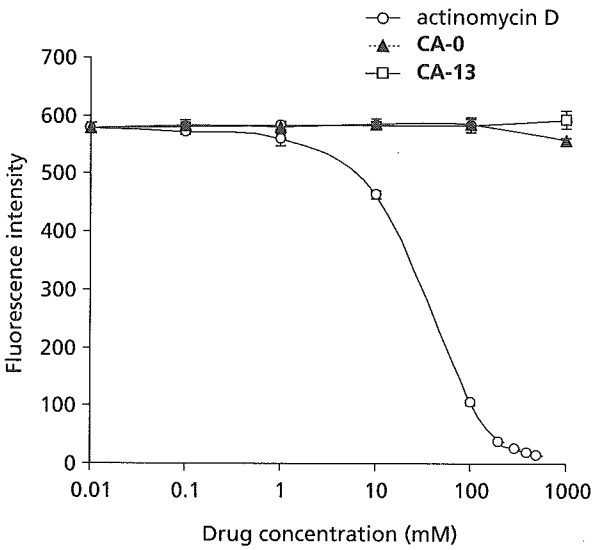

To evaluate intercalative activities of carbazole derivatives, ethidium bromide displacement assays were carried out for two representative compounds, **CA-0** and **CA-13**.

HeLa4.5/EGFP assay. Seven compounds exhibited considerable toxicity, suggesting that efforts toward decreasing toxicity are necessary for the further development of carbazole-based inhibitors.

Discussion

Carbazole, a fused phenyl-ring structure with hydrophobicity, has provided an interesting scaffold for the development of novel drugs. Staurosporine, discovered among microbial alkaloids, was the first carbazole derivative reported to demonstrate biological activity (Omura *et al.*, 1977; Furusaki *et al.*, 1978; Furusaki *et al.*, 1982), which was protein kinase C inhibition (Tamaoki *et al.*, 1986). Other carbazole derivatives have demonstrated various other activities, such as topoisomerase inhibition (Marotto *et al.*, 2002; Facompre *et al.*, 2002; Carrasco *et al.*, 2001), hypotensive activity (Furusaki *et al.*, 1982), platelet aggregation inhibition (Oka *et al.*, 1986), and anti-fungal activity (Sunthitikawinsakul *et al.*, 2003). In this report we present another possible activity of carbazole derivatives, that of HIV-1 integrase inhibitor.

As compounds with three or four fused aromatic ring structures have been reported to demonstrate intercalative activity (Fukui & Tanaka, 1996; Dziegielewski *et al.*, 2002), we initially suspected that our carbazole derivatives also have intercalative activities, penetrating and disturbing target dsDNA, resulting in pseudo strand-transfer inhibition. Indeed, several carbazole derivatives have been recognized to demonstrate intercalative activity (Facompre *et al.*, 2002; Long *et al.*, 2002). We confirmed that actinomycin D, which is a well-known intercalator (Ross *et al.*, 1979; Wilson & Jones, 1982), demonstrated strand-transfer inhibition in our assay (data not shown). However, taking into consideration the data that our carbazole derivatives inhibited strand-transfer in a competitive manner, and also that the compounds could not displace EtBr out from dsDNA, we assume that our derivatives bind to part of the IN molecule, to the region responsible for DNA target

binding or to the catalytic site responsible for strand-transfer activity.

To understand in greater detail the substituents responsible for strand-transfer inhibitory activity, we analysed 23 carbazole derivatives, and classified them into three categories according to their levels of inhibition (Table 1). Six compounds were classified as the high-inhibition group, which demonstrated IC_{50} of less than 10 μM, 12 compounds were classified as the intermediate group, which demonstrated IC_{50} of greater than 10 μM and less than 100 μM, and five compounds were classified as the non-inhibition group, in which we did not observe significant inhibition even at the highest concentration tested (100 μM).

Comparing the compounds between and within these three categories, we recognized three factors responsible for strand-transfer inhibition. The first and most important factor is the incidence of a 2-dimethylaminoethyl group at position R2 (Figure 1A).

CA-8, which possesses a 2-dimethylaminoethyl group at position R2, demonstrated high inhibitory activity (IC_{50}: 6.61 ±4.17 μM), but **CA-19** (IC_{50}: >100 μM), which possesses a phenyl ring structure at the same R2 position, did not demonstrate inhibitory activity. Thus, it is clear that the incidence of a 2-dimethylaminoethyl group, which has a basic property, is critical for strand-transfer inhibition activity. Indeed, we recognized that all compounds in the "high-inhibitory group" and "intermediate-inhibitory group" had this basic substituent at position R2 (Table 1A, 1B, Figure 2). In contrast, three of five compounds in the "non-inhibitory group" had the phenyl ring structure at R2 position. It is thought that these compounds might bind to the acidic region on the IN molecule and compete with the target dsDNA.

The second factor is the incidence of a methyl (Me) group at position R5, R6 or R7. We recognized that compounds in the high inhibitory group had at least one Me group at the R5, R6 or R7 position (Table 1A, Figure 2). Comparing **CA-1** (IC_{50}: 7.94 ±4.12 μM), **CA-4** (IC_{50}: 8.99 ±3.39 μM), and **CA-12** (IC_{50}: 5.93 ±3.53 μM) with **CA-15** (IC_{50}: 27.28 ±9.10 μM), it is clear that the incidence of an Me group within the R5 to R7 positions was an important factor for enhanced inhibitory activity. It seems that the position of the substituent may not be critical between R5 and R6, as we did not see significant differences between **CA-1** (IC_{50}: 7.94 ±4.12 μM) and **CA-12** (IC_{50}: 5.93 ±3.53 μM), and also between **CA-8** (IC_{50}: 6.61 ±4.17 μM) and **CA-9** (IC_{50}: 4.42 ±1.87 μM).

According to the IC_{50} levels of **CA-5** (>100 μM), **CA-6** (>100 μM) and **CA-11** (>100 μM), it appears that bulky substituents at the R5 position have a negative effect on inhibition (Table 1C, Figure 2). Furthermore, the inhibition potential of the three compounds **CA-1** (IC_{50}: 7.94 ±4.12 μM), **CA-16** (IC_{50}: 20.51 ±15.11 μM) and **CA-17** (IC_{50}: 50.64 ±19.02 μM) depended on the molecular size of their R5 substituents. It is probable that the R5 substituents of these compounds were too large and that they interfered with surrounding molecules forming the binding site (Table 1A, 1B, Figure 2). These data indicate that the binding site of carbazole might have a space limitation, and thus the size and shape of the molecules may be important factors for inhibitor activity.

The third factor is the substituent at position R9. Comparing **CA-20** (IC_{50}: >100 μM), **CA-21** (IC_{50}: 25.01 ±10.60 μM) and **CA-22** (IC_{50}: 16.92 ±7.32 μM), these three compounds were identical, with the exception of the substituent at position R9 (Table 1B, 1C, Figure 2). **CA-21** and **CA-22** have hydroxyl residue and a methoxy group at position R9, respectively. We noticed a significant difference in inhibitory activity between **CA-20** and **CA-21**, and between **CA-20** and **CA-22**, suggesting the possibility that both the hydroxyl group and the methoxy group at R9 formed hydrogen bonds with the amino acid molecules forming the binding sites, as these two substituents have the potential to be hydrogen bond acceptors. It appears that hydroxyl and methoxy groups have similar effects on strand-transfer inhibitory activities. In addition to the above three factors, we found that molecular interaction between R8 and R9 substituents, and their arrangement, are also important determinants for efficient inhibitory activity. **CA-3**, with two methoxy groups at R8 and R9, appears to have a bulky arrangement of the two side chains, and demonstrated an IC_{50} of 72.69 ±5.44 μM, whereas **CA-14** and **CA-18**, which were expected to have horizontal arrangements, demonstrated lower IC_{50} values of 17.37 ±1.79 μM and 10.68 ±8.88 μM, respectively (Table 1B, Figure 2).

To summarize these structural elements, and to understand the common structure of molecules that demonstrated strand-transfer inhibitory activity, we superposed inhibitor structures having significant strand-transfer inhibition (**CA-0**, **CA-1**, **CA-4**, **CA-8**, **CA-9**, **CA-12** and **CA-13**) (Figure 5A), and the structures of compounds with no inhibition (**CA-5**, **CA-6**, **CA-10**, **CA-19** and **CA-20**) (Figure 5B). In comparing these two overlapped figures, we found that the compounds with inhibitory activity share a largely identical structure and similar molecular size. In contrast, the non-inhibitory compounds had larger and more uneven-shaped side chains. Overall, the superposed structures indicate that the molecules should be planar and have basic diethylaminoethyl groups to demonstrate strand-transfer inhibitory activity.

In conclusion, we have identified a small molecular weight compound with a carbazole scaffold, which can be the lead compound for developing novel IN inhibitors. Furthermore, analysing the IN inhibitory mechanisms of

Figure 5. A structural comparison between high/intermediate inhibitory compounds and non-inhibitory compounds

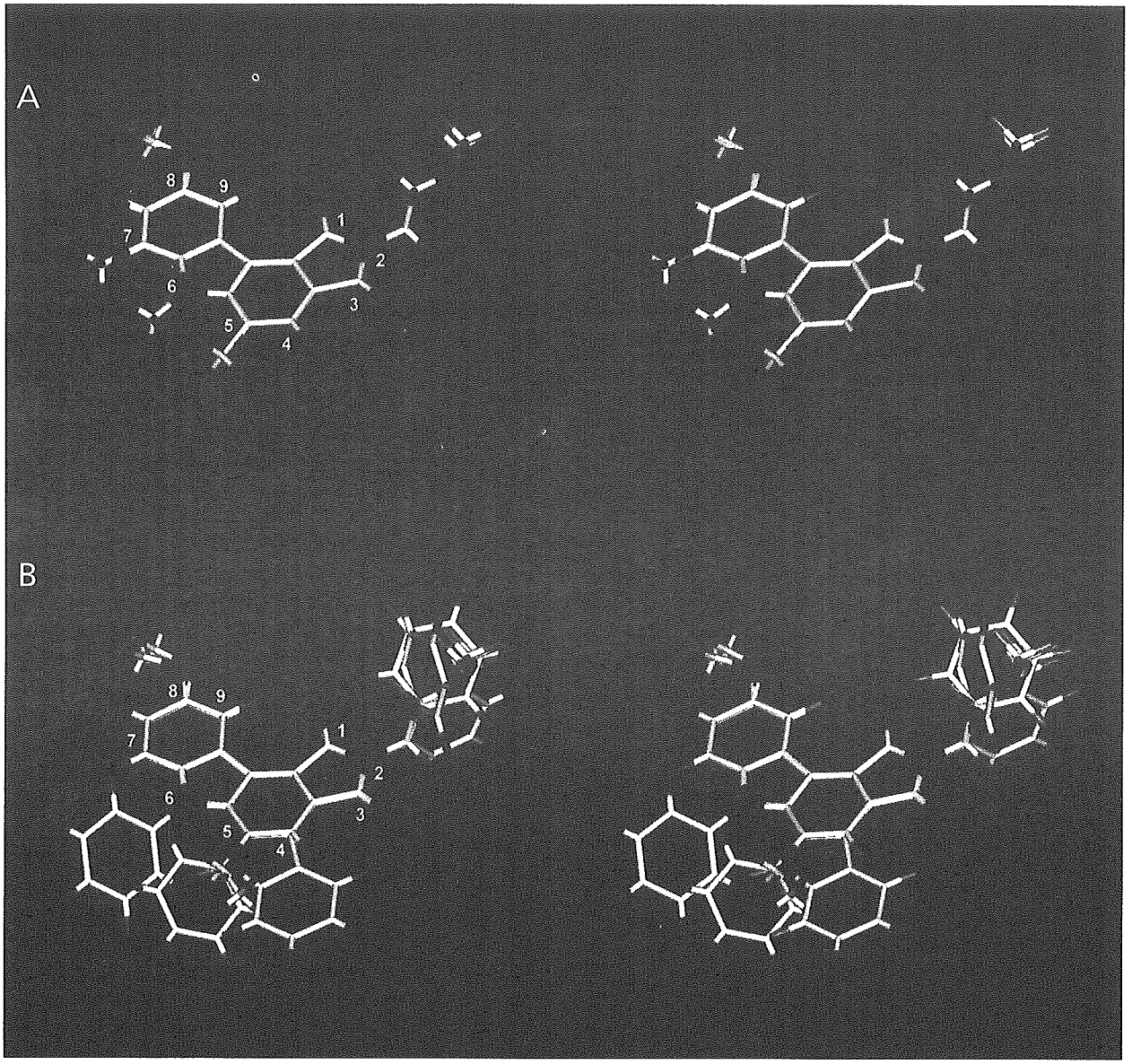

Superposed structures of **(A)** five non-inhibitory compounds, **CA-5**, **6**, **10**, **19** and **20**, and **(B)** seven inhibitory compounds, **CA-0**, **1**, **4**, **8**, **9**, **12** and **13**, are demonstrated in stereo-view images. In both figures, residue numbers are indicated beside the structures. Red, dark blue and light blue indicate oxygen, nitrogen and hydrogen molecules, respectively. Green indicates chlorine or fluorine molecules. SYBYL software Version 6.9.1 running on an SGI Fuel workstation was used to construct the figures.

carbazole derivatives may yield more detailed information regarding HIV-1 IN structure and function.

Acknowledgements

This study was supported by a grant from the Human Sciences Foundation, the Organization of Pharmaceutical Safety and Research of Japan and the Ministry of Health, Labor and Welfare of Japanese Government. This study was partly supported by the Program for Promotion of Fundamental Studies in Health Sciences of the National Institute of Biomedical Innovation (NIBIO)

We would like to thank Dr. Haruo Tanaka and Takuro Shiomi, professor and associate professor of Kitazato

Institute, for their valuable advice and comments. We would also like to thank the laboratory members of Toyama Chemical Co. Ltd. for supplying the compounds in the study. Finally, we would like to thank Ms. Mary Phillips and Ms. Yumi Fujiuji for preparing the manuscript.

References

Balzarini J (2004) Current status of the non-nucleoside reverse transcriptase inhibitors of human immunodeficiency virus type 1. *Current Topics in Medicinal Chemistry* **4**:921–944.

Burke CJ, Sanyal G, Bruner MW, Ryan JA, LaFemina RL, Robbins HL, Zeft AS, Middaugh CR & Cordingley MG (1992) Structural implications of spectroscopic characterization of a putative zinc finger peptide from HIV-1 integrase. *The Journal of Biological Chemistry* **267**:9639–9644.

Cain BF, Baguley BC & Denny WA (1978) Potential antitumor agent. 28. deoxyribonucleic acid polyintercalating agents. *Journal of Medicinal Chemistry* **21**:658–668.

Carrasco C, Vezin H, Wilson WD, Ren J, Chaires JB & Bailly C (2001) DNA binding properties of the indolocarbazole antitumor drug NB-506. *Anticancer Drug Design* **16**:99–107.

Chun TW, Finzi D, Margolick J, Chadwick K, Schwartz D & Siliciano RF (1995) *In vivo* fate of HIV-1-infected T cells: quantitative analysis of the transition to stable latency. *Nature Medicine* **1**:1284–1290.

Craigie R, Hickman AB & Engelman A (1995) Integrase. in *HIV: A Practical Approach – Volume 2: Biochemistry, Molecular Biology, and Drug Discovery*; pp. 53–71. Edited by J Karn. New York: Oxford University Press.

Dayam R & Neamati N (2003) Small-molecule HIV-1 integrase inhibitors: the 2001–2002 update. *Current Pharmacology Design* **9**:1789–1802.

De Clercq E (1992) HIV inhibitors targeted at the reverse transcriptase. *AIDS Research and Human Retroviruses* **8**:119–134.

Dziegielewski J, Slusarski B, Konitz A, Skladanowski A & Konopa J (2002) Intercalation of imidazoacridinones to DNA and its relevance to cytotoxic and antitumor activity. *Biochemical Pharmacology* **63**:1653–1662.

Engelman A & Craigie R (1992) Identification of conserved amino acid residues critical for human immunodeficiency virus type 1 integrase function *in vitro*. *Journal of Virology* **66**:6361–6369.

Engelman A, Englund G, Orenstein JM, Martin MA & Craigie R (1995) Multiple effects of mutations in human immunodeficiency virus type 1 integrase on viral replication. *Journal of Virology* **69**:2729–2736.

Engelman A, Hickman AB & Craigie R (1994) The core and carboxyl-terminal domains of the integrase protein of human immunodeficiency virus type 1 each contribute to nonspecific DNA binding. *Journal of Virology* **68**:5911–5917.

Facompre M, Carrasco C, Colson P, Houssier C, Chisholm JD, Van Vranken DL & Bailly C (2002) DNA binding and topoisomerase I poisoning activities of novel disaccharide indolocarbazoles. *Molecular Pharmacology* **62**:1215–1227.

Fukui K & Tanaka K (1996) The acridine ring selectively intercalated into a DNA helix at various types of abasic sites: double strand formation and photophysical properties. *Nucleic Acids Research* **24**:3962–3967.

Furusaki A, Hashiba N, Matsumoto T, Hirano A, Iwai Y & Omura S (1978) X-ray crystal structure of staurosporine: a new alkaloid from a Streptomyces strains. *Journal of the Chemical Society. Chemical Communications* 800–801.

Furusaki A, Hashiba N, Matsumoto T, Hirano A, Iwai Y & Omura S (1982) The crystal and molecular structure of staurosporine, a new alkaloid from a Streptomyces strains. *Bulletin of the Chemical Society of Japan* **55**:3681–3685.

Goldgur Y, Craigie R, Cohen GH, Fujiwara T, Yoshinaga T, Fujishita T, Sugimoto H, Endo T, Murai H & Davies DR (1999) Structure of the HIV-1 integrase catalytic domain complexed with an inhibitor: a platform for antiviral drug design. *Proceedings of the National Academy of Sciences, USA* **96**:13040–13043.

Grobler JA, Stillmock K, Hu B, Witmer M, Felock P, Espeseth AS, Wolfe A, Egbertson M, Bourgeois M, Melamed J, Wai JS, Young S, Vacca J & Hazuda DJ (2002) Diketo acid inhibitor mechanism and HIV-1 integrase: implications for metal binding in the active site of phosphotransferase enzymes. *Proceedings of the National Academy of Sciences USA* **99**:6661–6666.

Hazuda DJ, Anthony NJ, Gomez RP, Jolly SM, Wai JS, Zhuang L, Fisher TE, Embrey M, Guare JP, Jr., Egbertson MS, Vacca JP, Huff JR, Felock PJ, Witmer MV, Stillmock KA, Danovich R, Grobler J, Miller MD, Espeseth AS, Jin L, Chen IW, Lin JH, Kassahun K, Ellis JD, Wong BK, Xu W, Pearson PG, Schleif WA, Cortese R, Emini E, Summa V, Holloway MK & Young SD (2004) A naphthyridine carboxamide provides evidence for discordant resistance between mechanistically identical inhibitors of HIV-1 integrase. *Proceedings of the National Academy of Sciences USA* **101**:11233–11238.

Hazuda DJ, Felock P, Witmer M, Wolfe A, Stillmock K, Grobler JA, Espeseth A, Gabryelski L, Schleif W, Blau C & Miller MD (2000) Inhibitors of strand transfer that prevent integration and inhibit HIV-1 replication in cells. *Science* **287**:646–650.

Imamichi T (2004) Action of anti-HIV drugs and resistance: reverse transcriptase inhibitors and protease inhibitors. *Current Pharmaceutical Design* **10**:4039–4053.

Johnson AA, Marchand C & Pommier Y (2004) HIV-1 integrase inhibitors: a decade of research and two drugs in clinical trial. *Current Topics in Medicinal Chemistry* **4**:1059–1077.

Khan E, Mack JP, Katz RA, Kulkosky J & Skalka AM (1991) Retroviral integrase domains: DNA binding and the recognition of LTR sequences. *Nucleic Acids Research* **19**:851–860.

Kohl NE, Emini EA, Schleif WA, Davis LJ, Heimbach JC, Dixon RA, Scolnick EM & Sigal IS (1988) Active human immunodeficiency virus protease is required for viral infectivity. *Proceedings of National Academy of Sciences USA* **85**:4686–4690.

LaFemina RL, Schneider CL, Robbins HL, Callahan PL, LeGrow K, Roth E, Schleif WA & Emini EA (1992) Requirement of active human immunodeficiency virus type 1 integrase enzyme for productive infection of human T-lymphoid cells. *Journal of Virology* **66**:7414–7419.

Long BH, Rose WC, Vyas DM, Matson JA & Forenza S (2002) Discovery of antitumor indolocarbazoles: rebeccamycin, NSC 655649, and fluoroindolocarbazoles. *Current Medicinal Chemistry. Anti-Cancer Agents* **2**:255–266.

Marotto A, Kim YS, Schulze E & Pindur U (2002) New indolocarbazoles as antitumour active compounds: evaluation of the target by experimental and theoretical studies. *Pharmazie* **57**:194–197.

Oka S, Kodama M, Takeda H, Tomizuka N & Suzuki H (1986) Staurosporine, a potent platelet aggregation inhibitor form a *Streptomyces* species. *Agricultural and Biological Chemistry* **50**:2723–2727.

Omura S, Iwai Y, Hirano A, Nakagawa A, Awaya J, Tsuchya H, Takahashi Y & Masuma R (1977) A new alkaloid AM-2282 of *Streptomyces* origin. Taxonomy, fermentation, isolation and preliminary characterization. *The Journal of Antibiotics (Tokyo)* **30**:275–282.

Pluymers W, Pais G, Van Maele B, Pannecouque C, Fikkert V, Burke TR, Jr., De Clercq E, Witvrouw M, Neamati N & Debyser Z (2002) Inhibition of human immunodeficiency virus type 1 integration by diketo derivatives. *Antimicrobial Agents and Chemotherapy* **46:**3292–3297.

Pommier Y, Marchand C & Neamati N (2000) Retroviral integrase inhibitors year 2000: update and perspectives. *Antiviral Research* **47:**139–148.

Ross WE, Glaubiger D & Kohn KW (1979) Qualitative and quantitative aspects of intercalator-induced DNA strand breaks. *Biochimica et Biophyssica Acta* **562:**41–50.

Ruscetti FW (1985) Immunopathology associated with human lymphotropic retroviruses. *Survey and Synthesis of Pathology Research* **4:**216–226.

Schauer M & Billich A (1992) The N-terminal region of HIV-1 integrase is required for integration activity, but not for DNA-binding. *Biochemical and Biophysical Research Communications* **185:**874–880.

Sunthitikawinsakul A, Kongkathip N, Kongkathip B, Phonnakhu S, Daly JW, Spande TF, Nimit Y & Rochanaruangrai S (2003) Coumarins and carbazoles from *Clausena excavata* exhibited antimycobacterial and antifungal activities. *Planta Medica* **69:**155–157.

Tamaoki T, Nomoto H, Takahashi I, Kato Y, Morimoto M & Tomita F (1986) Staurosporine, a potent inhibitor of phospho-lipid/Ca^{++} dependent protein kinase. *Biochemical and Biophysical Research Communications* **135:**397–402.

Tronchet JM & Seman M (2003) Non-nucleoside inhibitors of HIV-1 reverse transcriptase: from the biology of reverse transcription to molecular design. *Current Topics in Medicinal Chemistry* **3:**1496–1511.

Wilson WD & Jones RL (1982) Interaction of actinomycin D, ethidium, quinacrine, daunorubicin, and tetralysine with DNA: 31P NMR chemical shift and relaxation investigation. *Nucleic Acids Research* **10:**1399–1410.

Woerner AM & Marcus-Sekura CJ (1993) Characterization of a DNA binding domain in the C-terminus of HIV-1 integrase by deletion mutagenesis. *Nucleic Acids Research* **21:**3507–3511.

Received 22 August 2005, accepted 27 September 2005

Impact of HIV-1 Subtype and Antiretroviral Therapy on Protease and Reverse Transcriptase Genotype: Results of a Global Collaboration

Rami Kantor[1*¤], David A. Katzenstein[1], Brad Efron[2], Ana Patricia Carvalho[3], Brian Wynhoven[4], Patricia Cane[5], John Clarke[6], Sunee Sirivichayakul[7], Marcelo A. Soares[8], Joke Snoeck[9], Candice Pillay[10], Hagit Rudich[11], Rosangela Rodrigues[12], Africa Holguin[13], Koya Ariyoshi[14], Maria Belen Bouzas[15], Pedro Cahn[15], Wataru Sugiura[14], Vincent Soriano[13], Luis F. Brigido[12], Zehava Grossman[11], Lynn Morris[10], Anne-Mieke Vandamme[9], Amilcar Tanuri[8], Praphan Phanuphak[7], Jonathan N. Weber[6], Deenan Pillay[16], P. Richard Harrigan[4], Ricardo Camacho[3], Jonathan M. Schapiro[1], Robert W. Shafer[1]

1 Division of Infectious Disease and Center for AIDS Research, Stanford University, Stanford, California, United States of America **2** Department of Statistics and Division of Biostatistics, Stanford University, Stanford, California, United States of America **3** Hospital Egas Moniz, Lisbon, Portugal, **4** BC Centre for Excellence in HIV/AIDS, Vancouver, British Columbia, Canada, **5** Health Protection Agency, Porton Down, United Kingdom, **6** Wright Fleming Institute, Imperial College, St. Mary's Hospital, London, United Kingdom **7** Chulalongkorn University, Bangkok, Thailand, **8** Universidade Federal do Rio de Janeiro, Brazil, **9** Rega Institute for Medical Research, Leuven, Belgium, **10** National Institute of Communicable Diseases, Johannesburg, South Africa, **11** Central Virology, Public Health Laboratories, Ministry of Health, Tel-Hashomer, Israel, **12** Instituto Adolfo Lutz, Sao Paulo, Brazil, **13** Hospital Carlos III, Madrid, Spain, **14** National Institute of Infectious Diseases, Tokyo, Japan, **15** Fundación Huesped, Buenos Aires, Argentina, **16** University College London and Health Protection Agency, London, United Kingdom

Competing Interests: The authors have declared that no competing interests exist.

Author Contributions: See Acknowledgments.

Academic Editor: David D. Ho, The Rockefeller University, United States of America

Citation: Kantor R, Katzenstein DA, Efron B, Carvalho AP, Wynhoven B, et al. (2005) Impact of HIV-1 subtype and antiretroviral therapy on protease and reverse transcriptase genotype: Results of a global collaboration. PLoS Med 2(4): e112.

Received: October 8, 2004
Accepted: March 7, 2005
Published: April 26, 2005

DOI: 10.1371/journal.pmed.0020112

Abbreviations: NRTI, nucleoside reverse transcriptase inhibitor; NNRTI, non-nucleoside reverse transcriptase inhibitor; PI, protease inhibitor; RT, reverse transcriptase; RTI, reverse transcriptase inhibitor

*To whom correspondence should be addressed. E-mail: rkantor@brown.edu

¤Current affiliation: Division of Infectious Diseases, Brown University, Providence, Rhode Island, United States of America

ABSTRACT

Background

The genetic differences among HIV-1 subtypes may be critical to clinical management and drug resistance surveillance as antiretroviral treatment is expanded to regions of the world where diverse non-subtype-B viruses predominate.

Methods and Findings

To assess the impact of HIV-1 subtype and antiretroviral treatment on the distribution of mutations in protease and reverse transcriptase, a binomial response model using subtype and treatment as explanatory variables was used to analyze a large compiled dataset of non-subtype-B HIV-1 sequences. Non-subtype-B sequences from 3,686 persons with well characterized antiretroviral treatment histories were analyzed in comparison to subtype B sequences from 4,769 persons. The non-subtype-B sequences included 461 with subtype A, 1,185 with C, 331 with D, 245 with F, 293 with G, 513 with CRF01_AE, and 618 with CRF02_AG. Each of the 55 known subtype B drug-resistance mutations occurred in at least one non-B isolate, and 44 (80%) of these mutations were significantly associated with antiretroviral treatment in at least one non-B subtype. Conversely, of 67 mutations found to be associated with antiretroviral therapy in at least one non-B subtype, 61 were also associated with antiretroviral therapy in subtype B isolates.

Conclusion

Global surveillance and genotypic assessment of drug resistance should focus primarily on the known subtype B drug-resistance mutations.

Introduction

The HIV-1 pandemic resulted from the cross-species transmission of a lentivirus, most likely of chimpanzee origin, that began spreading among humans during the first half of the previous century [1,2,3]. The progeny of this zoonotic infection—designated HIV-1 group M (main) viruses—make up the vast majority of HIV-1 infections. During their spread among humans, group M viruses have developed an extraordinary degree of genetic diversity, and most can be segregated into nine pure subtypes and several commonly circulating recombinant forms [4].

HIV-1 subtype B is the predominant subtype in North America, Western Europe, and Australia. The antiretroviral drugs used to treat HIV were developed using biophysical, biochemical, and in vitro studies of subtype B isolates, and most data on the genetic mechanisms of HIV-1 drug resistance are from subtype B viruses. However, HIV-1 subtype B viruses account for only approximately 12% of the global HIV pandemic [5], and as therapy is introduced into developing countries, the number of persons with non-B viruses initiating therapy will increase dramatically.

HIV-1 subtypes differ from one another by 10%–12% of their nucleotides and 5%–6% of their amino acids in protease and reverse transcriptase (RT) [6]. Intersubtype nucleotide differences influence the spectrum of amino acid substitutions resulting from point mutations, and intersubtype amino acid differences influence the biochemical and biophysical microenvironment within the protease and RT [7,8]. These differences among subtypes therefore could influence the spectrum of mutations that develop during selective drug pressure.

An increasing number of observational studies, in vitro and in vivo, suggest that the currently available protease and RT inhibitors are as active against non-B viruses as they are against subtype B viruses [9,10,11,12,13,14,15,16,17,18,19,20,21,22,23,24,25,26]. However, fewer data are available on the genetic mechanisms of drug resistance in non-B viruses, and some in vitro and in vivo observations suggest that the various subtypes may respond differently to certain antiretroviral drugs [27,28,29,30,31,32,33,34,35].

Identifying the relevant drug-resistance mutations among non-B subtypes will be important for monitoring the evolution and transmission of drug resistance, for determining initial treatment strategies for persons infected with non-B viruses, and for interpreting genetic resistance among patients who fail antiretroviral therapy.

In this study, we characterize protease and RT mutations in non-B HIV-1 subtypes from persons receiving antiretroviral therapy, and attempt to answer the following two questions. (i) Do the mutations that cause drug resistance in subtype B viruses also develop in non-B viruses exposed to antiretroviral drugs? (ii) Do novel mutations emerge in non-subtype-B viruses during antiretroviral drug failure that are not recognized in subtype B viruses?

Methods

HIV-1 Sequences and Antiretroviral Treatments

Sequences of HIV-1 protease (positions 1–99) and RT (positions 1–240) from persons whose antiretroviral treatment history was known were collected from the published literature and from 14 laboratories in 12 countries. Persons were considered untreated if they had never been exposed to antiretroviral drugs, and treated if they were receiving RT inhibitors (RTIs) and/or protease inhibitors (PIs) at the time the isolate was obtained. Sequences from treated persons were included for analysis only if they were obtained from persons whose entire treatment histories were known. If multiple isolates from the same person were sequenced, only the latest isolate was included for analysis. Only sequences determined using dideoxyterminator sequencing were included in the analysis. In all, 99% of sequences were determined using direct PCR (population-based sequencing), and 1% of sequences represented the consensus sequence of multiple clones.

Samples obtained from patients were submitted to clinical and research laboratories for resistance testing in the course of evaluation and care of HIV infection. Data analyzed included published and presented data obtained under protocols approved by national and local institutional review boards or ethical review panels in each country. Sequence, demographic, and treatment data, unlinked from all personal identifiers, were analyzed at Stanford University under a protocol approved by the Stanford University Panel on Human Subjects.

Subtype Assignment

Similarity plotting and bootscanning using a window size of 400 nucleotides and a step size of 40 nucleotides were performed using reference sequences for each of the nine pure subtypes (A, B, C, D, F, G, H, J, and K) and two recombinant forms (CRF01_AE and CRF02_AG) [36]. Isolates that contained a combination of more than one subtype were excluded from analysis, except when subtypes A and G were detected in a pattern consistent with CRF02_AG. Because CRF01_AE *pol* sequences do not contain recombinant breakpoints, subtype assignment was based on the fact that *pol* CRF01_AE and pure A sequences are divergent. This approach had an accuracy of 96% when applied to the protease and RT genes of 137 well characterized subtype A, CRF01_AE, and CRF02_AG isolates with known subtypes based on *pol* and *gag* and/or *env*, with most errors resulting from the misclassification of subtype A protease sequences as CRF01_AE (data not shown).

Reference sequences used were U455 (subtype A), CM240 (CRF01_AE), IbNG (CRF02_AG), HXB2 (subtype B), C2220 (subtype C), NDK (subtype D), 93BR020 (subtype F), SE6165 (subtype G), 90CR056 (subtype H), SE9173c (subtype J), 97EQTB11C (subtype K), YBF30 (Group N), and ANT70C (Group O). A total of 223 protease and 307 RT sequences of indeterminate subtype were excluded from the analysis.

Mutation Definitions

Each sequence was translated and compared to the consensus B protease and RT sequences in the Los Alamos HIV Sequence database (http://hiv-web.lanl.gov) using the HIVSeq program [37]. Mutations were defined as differences from the wild-type consensus B sequence. Known subtype B drug-resistance mutations were defined as follows: 18 nucleoside RTI (NRTI)-resistance positions at 41, 44, 62, 65, 67, 69, 70, 74, 75, 77, 115, 116, 118, 151, 184, 210, 215, and 219; 15 non-nucleoside RTI (NNRTI)-resistance positions at 98, 100,